Optics Communications 387 (2017) 303–309

Contents lists available at ScienceDirect

Optics Communications

journal homepage: www.elsevier.com/locate/optcom

Interferogram stitching method in measuring the form deviation of curved surface with laser interferometry

Pengcheng Yang[a,*], Yang Liu[a], Suping Fang[b], Xindong Zhu[b], Guangshen Xu[a], Yuan Xiao[a]

[a] Mechanical and Electrical Engineering College, Xi'an Polytechnic University, Xi'an 710048, China
[b] State Key Laboratory of Manufacturing Systems Engineering, Xi'an Jiaotong University, Xi'an 710049, China

ARTICLE INFO

Keywords:
Stitching method
Interferogram
Surface shape
Laser interferometry

ABSTRACT

When the form deviation of curved surface is measured with oblique laser interferometry, the dense fringes are almost inevitable and prevent a high processing accuracy. This paper focuses on a stitching method to solve the problem: firstly, the reliable area in interferogram is evaluated according to the fringe width. Secondly, all interferograms are positioned on the measured surface which is regarded as the stitching reference. Thirdly, the transform models of different interferograms are estimated based on the same center of optical axis. Fourthly, the form deviations from different reliability areas are resampled. The experimental results are given to verify the feasibility.

1. Introduction

When laser interferometry is employed to measure the surface shape of the object, the interference fringe pattern (IFP) is the only collected measurement data, so its quantity is the key point for a high precision measurement [1]. Based on the improved Mach-Zehnder interferometer, the curved surface such as tooth flank of helical gear is irradiated and its IFP is collected [2]. When the helical angle or face width of measured helical gear is large, the optical path differences between the object path and the reference path vary greatly in curved surface. In the center of optical axle, the optical path difference changes slowly and the interference fringe is the widest. However, away from the center of optical axle, the optical path difference changes rapidly and the interference fringe is narrow, as shown in Fig. 1. The interference fringes in the tip and root areas are denser than the fringes in the middle area. According to the previous research, the processing accuracy of phase-shifting IFP is in inverse proportion to the fringe width, and is unreliable in the area where the fringe width is less than four pixels [3]. The lower processing accuracy will prevent the micron-level measurement accuracy, and limits the application of oblique laser interferometry. Moreover, the dense interference fringes are almost inevitable in actual measurement, so how to obtain the correct phase information in the dense fringe area is a key point in the oblique laser Interferometry. However, little research has been done on this issue.

In the beginning of the century, the researchers have proposed a method to modulate the density of interference fringe [4]. A spherical concave lens is added in the optical path of the reference beam over the CCD. By selecting a suitable focal length of the inserted concave lens, the optical path difference between the reference path and the object path becomes fairly small over the CCD image sensor. This method can reduce the fringe density of the IFP, but it needs to select the focal length of lenses in accordance with the different shapes of measured surfaces. It is only applied in the measurement of specialized surface. When the measured surface has a variety of shapes and sizes, the modulation lens needs to be changed frequently. Moreover, these high precision lenses will be high cost. Thus, the previous research is not very satisfactory, and further studies are still necessary.

In the experiment, the position of the widest fringe can be shifted by adjusting the rotation angle of the reflector in optical system. Therefore, a stitching method is considered: firstly, the local sparser fringe which meets the processing accuracy will be distinguished; secondly, these local sparer fringes will be stitched and the form deviation of completed measured surface is expected.

During the past decades, a lot of stitching methods have emerged in the field of image processing [5,6]. In these stitching algorithms, firstly the corresponding relationship of different images will be established by feature points. Generally, the feature detection method can be divided into Ares-based method and Feature-based method [7]. Area-based methods, sometimes called correlation-like methods or template matching. Windows of predefined size or even entire images are used for the correspondence estimation [7,8]. In actual measurement, the distribution of all interference fringes changes with the movement of the widest fringe, therefore the correspondence estimation cannot be

* Corresponding author.
E-mail address: pcyang0@gmail.com (P. Yang).

http://dx.doi.org/10.1016/j.optcom.2016.11.077
Received 7 October 2016; Received in revised form 25 November 2016; Accepted 29 November 2016
0030-4018/ © 2016 Elsevier B.V. All rights reserved.

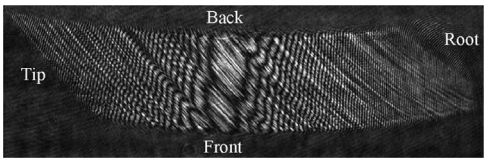

Fig. 1. The collected IFP of helical gear tooth flank.

applied for the IFP. Feature-based method is based on the extraction of salient structures–features in the images, such as significant areas, lines or points [7,9]. From Fig. 1, the IFP is different with the digital photos in our daily life, it is anamorphic and image foreshortened and there is no salient feature could be detected, so the Feature-based method is also difficult to be used. Moreover, the different IFPs have the different centers of optical axle, and the calculated form deviations are not in the same coordinate system, thus they cannot be just stitched. This paper will propose a stitching method for the IFP to solve the problem.

The stitching method of IFP is elaborated upon in Section 2. In Section 3, the experiments are performed and discussed. Section 4 is the conclusion.

2. Stitching method for IFP

The proposed stitching method is composed of four steps: 1. Registration between actual tooth flank and IFP; 2. Reliability evaluation based on fringe width; 3. Transform model estimation; 4. Image resampling.

First of all, the tooth flank of helical gear is the measured surface, and its measurement coordinate system shown in Fig. 2 is introduced. The measured tooth flank is divided into W parts in the direction of tooth width and H parts in the direction of tooth height evenly, and W and H are positive integers. So there are $(W + 1) \times (H + 1)$ grid points in tooth flank as shown in Fig. 3. Any grid point is denoted as $G(h, w)$, $h = 0, 1, \ldots, H$ and $w = 0, 1, \ldots, W$, and its spatial coordinate value is $\mathbf{D}_{(h,w)}$. The three-dimensional vector $\mathbf{n}$ is the normal direction of grid point, for example the normal direction of grid points $G(h, w)$ is $\mathbf{n}_{(h,w)}$. All symbols in the paper are listed in Table 1.

2.1. 1 IFP registration

In stitching method, a stitching reference for all IFPs is necessary. Though the fringe distributions are different in each group of IFP, they map the same measured tooth flank. Based on the mapping relationship, the measured tooth flank is regarded as the reference plane in stitching method. The form deviations from IFPs will be positioned on the actual tooth flank firstly before IFPs stitching.

Because the IFP is anamorphic distortion and image foreshortening in the oblique incidence interferometry, it cannot be positioned on the

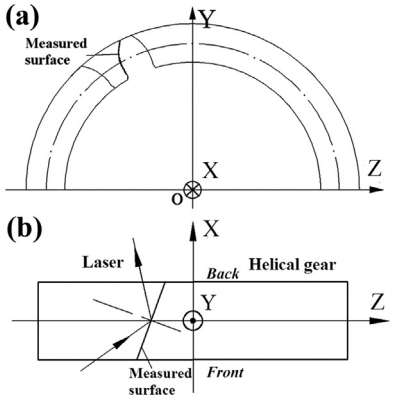

Fig. 2. The coordinate system of the measured helical gear.

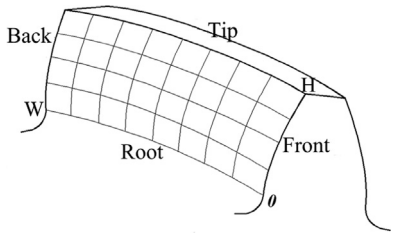

Fig. 3. The grid points of the tooth flank.

Table 1
The symbols list.

Symbols	*Instructions*
IFP	Interference fringe pattern
STI	Simulated tooth image
PSD	Pseudocorrelation
W	The division numbers in the direction of tooth width
H	The division numbers in the direction of tooth height
$G(h, w)$	The grid point in actual tooth flank, $h = 0, 1, \ldots, H$, $w = 0, 1, \ldots, W$
$\mathbf{D}_{(h,w)}$	The spatial coordinate value of grid point $G(h, w)$
$\mathbf{n}_{(h,w)}$	The normal direction of grid points $G(h, w)$
$S(h, w)$	The simulated tooth point
$I(h, w)$	The pixel point mapping with the grid points $G(h, w)$ in the IFP
k	The size of a kernel matrix in the PSD
Γ_{PSD}	The threshold to determine the reliable area
f	The optical path difference before the coordinate transformation
f'	The optical path difference after the coordinate transformation
$\mathbf{N}$	The three-dimensional matrix used in the coordinate transformation
$\mathbf{k}$	The normal direction of the plane composed by $\mathbf{n}_{(H/2,W/2)}$ and $\mathbf{n}_{(h_0,W/2)}$
$R(h, w)$	The reliable form deviation
$L(h, w)$	The overlapped form deviation
$B(w)$	A array instructs the location of boundary points

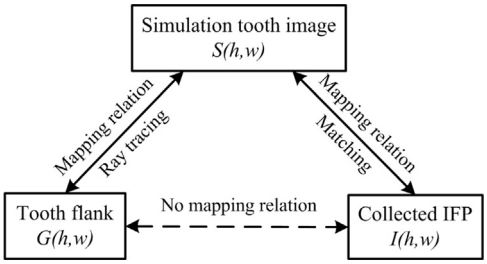

Fig. 4. The registration procedure.

measured tooth flank directly and a registration method is employed [10]. Firstly, the registration method shown in Fig. 4 will be introduced briefly.

For every grid point on measured tooth flank, the ray tracing is carried out until ending with the CCD sensor in optical measurement system. So every grid point $G(h, w)$ maps a simulated imaging point on the CCD sensor. These simulated imaging points are denoted as $S(h, w)$, and compose the simulated tooth image (STI) as shown in Fig. 5. Then, the STI is transformed (including translational motion, rotation and enlargement etc.) to match with the IFP, so every simulated tooth point $S(h, w)$ maps a point denoted as $I(h, w)$ in the collected IFP. Finally, the STI bridges the collected IFP and the actual tooth flank.

With the help of the registration method, the shape information from IFP can be restored to the actual tooth flank, and gets ready for the next step.

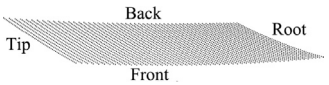

Fig. 5. The simulation tooth image.

Download English Version:

https://daneshyari.com/en/article/5449720

Download Persian Version:

https://daneshyari.com/article/5449720

Daneshyari.com